Journal of Beijing Institute of Technology, 2021, Vol. 30, Suppl.1

Hypersonic Re-entry Vehicle Fault-Tolerant Control Against Actuator Failure via Integral Sliding Mode

Fuhui Guo[1,2] and Pingli Lu[1,2,✉]

(1. School of Automation, Beijing Institute of Technology, Beijing 100081, China; 2. State Key Laboratory of Intelligent Control and Decision of Complex Systems, Beijing 100081, China)

Abstract: A fault-tolerant control (FTC) scheme is proposed based on integral sliding mode (ISM) for attitude control of hypersonic re-entry vehicle (HRV) under partial loss of actuator effectiveness. First, the inner/outer loop mathematical model of HRV in the present of actuator failure is given with specific analysis on torque. Then prescribed performance approach is introduced to the ISM controller design by error transformation. Specifically, the transformation error rather than tracking error is chosen as the sliding variable to establish the sliding mode surface and reaching law. As a result, the attitude tracking error of HRV is limited into the expected range. Meanwhile, the transient process and the steady state behavior are both considered. Considering that the unknown fault information of actuator can cause adverse effect on HRV, an extended state observer (ESO) is adopted to estimate the unknown actuator failure. Thus the observer result is served as compensation for the loss of the controlled system performance. Simulation results show that the proposed scheme can fulfil the tracking task with prescribed performance.

Key words: hypersonic re-entry vehicle; fault-tolerant control; actuator failure; prescribed performance function; integral sliding mode

CLC number: TP249.1 **Document code:** A **Article ID:** 1004-0579(2021)S1-0111-10

Highly nonlinearity of hypersonic re-entry vehicle (HRV) mathematical model and severe flight environment cause huge difficulty for controller design of HRV flight control system. Moreover, actuator failure, sensor fault and system failure also increase the difficulty of controller design. Therefore fault-tolerant control (FTC) is an important research direction in the field of HRV control as top priority[1]. Many scholars have worked on FTC among different faults for HRV based on sliding mode control (SMC) theory[2], back-stepping control[3], model predictive control (MPC)[4] and fuzzy control[5] and so forth. For instants, an adaptive FTC based on SMC is utilized for actuator failure by Zhai[2] to achieve tracking error converging to zero. For against actuator constraints, Hao et al.[3] has studied the FTC strategy combined with back-stepping for air-breathing HRV. In Ref.[4], MPC is employed to design a FTC controller when the actuator saturation is taken into consideration. Shen et al.[5] present a fault-tolerant controller based on Takagi-Sugeno fuzzy model.

Among the various nonlinear control methods, SMC theory is stick out for its strong robustness against unknown disturbance and brief design procedure. Moreover, SMC is also widely used for fault-tolerant control[6-10]. In Ref. [6], longitude model of the aircraft is studied when actuator failure and modeling uncertainties are taken

Received 2020-08-07
Supported by the National Natural Science Foundation of China (61433003, 60904003)
✉ Author for correspondence
E-mail: pinglilu@bit.edu.cn
DOI: 10.15918/j.jbit1004-0579.20104

into consideration. By designing different parameters for the proposed sliding mode controller, the stability of fault-tolerant control system can be achieved. In Ref. [7], a super-twisting sliding mode controller is carried out for HRV with actuator failure, and the control gain is designed with an adaptive form in order to compensate the failure. Thus the super-twisting SMC succeeds in attitude control. An integral terminal sliding mode control is designed in Ref. [8] by Peng et al. to deal with the faulty system of hypersonic gliding vehicle, and the controller could provide the faulty system finite-time stability in the presence of actuator failure. Ming et al.[9] investigate a FTC approach to control the supersonic-missile attitude dynamics when the actuator presents a typical loss of effectiveness, and an extended state observer is adopted to estimate the loss of actuator. In Ref. [10], the loss of effectiveness of the actuator is discussed, and adaptive dynamic sliding mode(ADSM) fault-tolerant control strategy is proposed. Based on the SMC, the above FTC strategies perform well, but it is not enough for the special features of HRV, specially the fast time-varying characteristics. Therefore, fault-tolerant control system needs to focus on both the transient performance and the steady state behavior.

On the basis of the requirement on the transient and steady-state behavior, a prescribed performance concept is adopted when designing the FTC controller[11-12]. The prescribed performance function (PPF) is firstly proposed by Bechlioulis et al. [11-12], which can improve both the transient and the steady state performance by transforming the tracking error into a prescribed performance bound. Then many scholars[13-15] apply prescribed performance function into their research fields and many research results have been established. Liu et al.[13] design the FTC controller combined with PPF for hypersonic flight vehicles with faulty and hysteretic actuators. In Ref. [14], PPF is used to constrain vertical displacement of the car-body from two aspects, that is, the maximum overshoot and the tracking error convergence. Li et al. [15] combine PPF with back-stepping control to ensure prescribed convergence overshoot and steady-state error.

Therefore, aiming at the aforementioned analysis, the primary contributions of the paper are summarized as follows.

A robust fault-tolerant strategy is designed for attitude control of HRV faulty system based on integral sliding mode in this paper. By adopting the PPF cooperated with ISM and ESO, the faulty system can obtain the twofold superior performance.

① The transient behavior and steady-state behavior of the faulty system are both considered.

② The attitude tracking error can be limited in a smaller prescribed residual range in spite of the unknown failure.

The rest of the paper is organized as follows. The dynamics of HRV are introduced under the actuator failure in the form of inner-outer loop in Section 1. In Section 2, the robust controller and the fault-tolerant controller are given based on ISM with PPF in detail. In addition, the stability of the faulty HRV system is guaranteed by Lyapunov stability theory. Simulation results are illustrated in Section 3. Section 4 concludes the paper.

1 Problem Statement

1.1 HRV dynamics under actuator failure

In this section, the dynamics equation of rotation motion and kinematic equation of HRV developed by NASA Langley Research Center[16] are given as follows:

$$\begin{cases} \dot{\alpha} = q - \tan\beta(p\cos\alpha + r\sin\alpha) + \\ \qquad \dfrac{1}{mV\cos\beta}(-L + mg\cos\gamma cos\mu) \\ \dot{\beta} = p\sin\alpha - r\cos\alpha + \dfrac{1}{mV}(Y + mg\cos\gamma\sin\mu) \\ \dot{\mu} = \sec\beta(p\cos\alpha + r\sin\alpha) + \\ \qquad \dfrac{1}{mV}(L\tan\beta + L\tan\gamma\sin\mu + \\ \qquad Y\tan\gamma\cos\mu - mg\cos\gamma\cos\mu\tan\beta) \end{cases} \tag{1}$$

$$\begin{cases} \dot{p} = \dfrac{I_{zz}}{I^*}M_x + \dfrac{I_{xz}}{I^*}M_z + \dfrac{(I_{xx}-I_{yy}+I_{zz})I_{xz}}{I^*}pq + \\ \qquad \dfrac{(I_{yy}-I_{zz})I_{zz}-I_{xz}^2}{I^*}qr \\ \dot{q} = \dfrac{1}{I_{yy}}M_y + \dfrac{I_{xz}}{I_{yy}}(r^2-p^2) + \dfrac{I_{zz}-I_{xx}}{I_{yy}}pr \\ \dot{r} = \dfrac{I_{xz}}{I^*}M_x + \dfrac{I_{xx}}{I^*}M_z + \dfrac{(I_{xx}-I_{yy})I_{xx}+I_{xz}^2}{I^*}pq + \\ \qquad \dfrac{(-I_{xx}+I_{yy}-I_{zz})I_{xz}}{I^*}qr \end{cases} \tag{2}$$

where α, β and μ denote angle of attack, sideslip angle and bank angle respectively. p, q, r denote the body angular rate, that is, roll angular rate, pitch angular rate and yaw angular rate. V is the velocity of HRV. γ is the flight path angle. L, Y are lift force and lateral force, respectively. m is the mass and g is the gravitational acceleration. M_x, M_y, M_z represent aerodynamic moment, that is, the roll, pitch and yaw torques which are defined in the body frame respectively. I_x, I_y, I_z denote moment of inertia of corresponding coordinate axes respectively and $I^* = I_{xx}I_{zz} - I_{xz}^2$.

Given that the dynamic responses of state variables α, β, μ and p, q, r are obviously different in time scales, thus state variables α, β, μ and p, q, r can be divided into two levels based on singular perturbation theory[17]. Specifically, α, β, μ are regarded as slow variable in outer loop, while p, q, r are regarded as quick variable in inner loop. Notice that translational motion of the HRV is much slower than its rotational motion, therefore the translational motion can be regarded as modeling uncertainties in attitude kinematics equation (Eq. (1)) [18]. Thus, Eqs. (1) (2) can be simplified as

$$\dot{\boldsymbol{x}}_1 = \boldsymbol{R}(\boldsymbol{x}_1)\boldsymbol{u}_1 + \boldsymbol{D} \tag{3}$$

$$\dot{\boldsymbol{x}}_2 = \boldsymbol{f}_2(\boldsymbol{x}_1, \boldsymbol{x}_2) + \boldsymbol{g}_2(\boldsymbol{x}_1, \boldsymbol{x}_2)\boldsymbol{M} \tag{4}$$

where $\boldsymbol{x}_1 = (\alpha, \beta, \mu)^{\mathrm{T}}$ is the state variable in outer loop. $\boldsymbol{x}_2 = (p, q, r)^{\mathrm{T}}$ is the state variable in inner loop, while $\boldsymbol{u}_1$ is the virtual control input for outer loop as well as reference signal $\boldsymbol{x}_{2,\mathrm{ref}}$ for inner loop. $\boldsymbol{D} = (d_1, d_2, d_3)^{\mathrm{T}}$. $d_1 = \dfrac{1}{mV\cos\beta}(-L + mg\cos\gamma\cos\mu)$, $d_2 = \dfrac{1}{mV}(Y + mg\cos\gamma\sin\mu)$, $d_3 = \dfrac{1}{mV}(L\tan\beta + L\tan\gamma\sin\mu + Y\tan\gamma\cos\mu - mg\cos\gamma\cos\mu\tan\beta)$

$\boldsymbol{M} = (M_{\mathrm{x}}, M_{\mathrm{y}}, M_{\mathrm{z}})^{\mathrm{T}}$

$$\boldsymbol{R}(x_1) = \begin{pmatrix} -\tan\beta\cos\alpha & 1 & -\tan\beta\sin\alpha \\ \sin\alpha & 0 & \cos\alpha \\ \sec\beta cos\alpha & 0 & \sec\beta sin\alpha \end{pmatrix}$$

$$\boldsymbol{g}_2 = \begin{pmatrix} I_{zz}/I^* & 0 & I_{xz}/I^* \\ 0 & 1/I_{yy} & 0 \\ I_{xz}/I^* & 0 & I_{xx}/I^* \end{pmatrix}$$

$\boldsymbol{f}_2 = (f_{21}, f_{22}, f_{23})^{\mathrm{T}}$

$f_{21} = (I_{xx} - I_{yy} + I_{zz})I_{xz}pq/I^* + ((I_{yy} - I_{zz})I_{zz} - I_{xz}^2)qr/I^*$

$f_{22} = I_{xz}(r^2 - p^2)/I_{yy} + (I_{zz} - I_{xx})pr/I_{yy}$

$f_{23} = ((I_{xx} - I_{yy})I_{xx} + I_{xz}^2)pq/I^* + (-I_{xx} + I_{yy} - I_{zz})I_{xz}qr/I^*$

As we all know, torque vector $\boldsymbol{M}$ is generated from two aspects as follows

$$\boldsymbol{M} = \boldsymbol{M}_{\mathrm{B}} + \boldsymbol{M}_{\delta} \tag{5}$$

On the one hand, the motion of airframe itself can generate torque $\boldsymbol{M}_{\mathrm{B}}$. On the other hand, the deflection of control rudder can also provide torque $\boldsymbol{M}_{\delta}$. The specific expressions of $\boldsymbol{M}_{\mathrm{B}}$ and $\boldsymbol{M}_{\delta}$ are given herein[16]

$$\boldsymbol{M}_{\mathrm{B}} = \begin{pmatrix} M_{\mathrm{B}x} \\ M_{\mathrm{B}y} \\ M_{\mathrm{B}z} \end{pmatrix} = \hat{q}S_{\mathrm{ref}} \begin{pmatrix} b & 0 & 0 \\ 0 & c & 0 \\ 0 & 0 & b \end{pmatrix} \cdot \begin{pmatrix} C_{\mathrm{m}x,\beta} + C_{\mathrm{m}x,\mathrm{p}}\dfrac{pb}{2V} + C_{\mathrm{m}x,\mathrm{r}}\dfrac{rb}{2V} \\ C_{\mathrm{m}y0} + C_{\mathrm{m}y,\mathrm{q}}\dfrac{qc}{2V} \\ C_{\mathrm{m}z,\beta}\beta + C_{\mathrm{m}z,\mathrm{p}}\dfrac{pb}{2V} + C_{\mathrm{m}z,\mathrm{r}}\dfrac{rb}{2V} \end{pmatrix} \tag{6}$$

$$\boldsymbol{M}_{\delta} = \begin{pmatrix} M_{x,\delta} \\ M_{y,\delta} \\ M_{z,\delta} \end{pmatrix} = \hat{q}S_{\mathrm{ref}} \begin{pmatrix} b & 0 & 0 \\ 0 & c & 0 \\ 0 & 0 & b \end{pmatrix} \cdot \begin{pmatrix} C_{\mathrm{m}x,\delta_{\mathrm{e}}} & C_{\mathrm{m}x,\delta_{\mathrm{a}}} & C_{\mathrm{m}x,\delta_{\mathrm{r}}} \\ C_{\mathrm{m}y,\delta_{\mathrm{e}}} & C_{\mathrm{m}y,\delta_{\mathrm{a}}} & C_{\mathrm{m}y,\delta_{\mathrm{r}}} \\ C_{\mathrm{m}z,\delta_{\mathrm{e}}} & C_{\mathrm{m}z,\delta_{\mathrm{a}}} & C_{\mathrm{m}z,\delta_{\mathrm{r}}} \end{pmatrix} \begin{pmatrix} \delta_{\mathrm{e}} \\ \delta_{\mathrm{a}} \\ \delta_{\mathrm{r}} \end{pmatrix} \tag{7}$$

where $C_{\mathrm{m}y0}, C_{\mathrm{m}x,*}, C_{\mathrm{m}y,*}, C_{\mathrm{m}z,*}$ (The subscript $*$ denotes $\delta_{\mathrm{e}}, \delta_{\mathrm{a}}, \delta_{\mathrm{r}}, \beta, p, q, r$) represent the moment coefficients. $\delta_{\mathrm{e}}, \delta_{\mathrm{a}}, \delta_{\mathrm{r}}$ denote the deflections of elevator, aileron and rudder respectively. b, c, S_{ref} represent the configuration parameters of vehicle[16]. $\hat{q} = \rho_{\mathrm{a}}V^2/2$ denotes the dynamic pressure, ρ_{a} is the atmospheric density.

Substituting Eqs. (5) – (7) into Eq. (4), it can be obtained that

$$\dot{\boldsymbol{x}}_2 = \boldsymbol{f}_{2\mathrm{f}} + \boldsymbol{g}_{2\mathrm{f}}\boldsymbol{u}_2 \tag{8}$$

where $\boldsymbol{u}_2$ is control input, $\boldsymbol{u}_2=(\delta_{\mathrm{e}},\delta_{\mathrm{a}},\delta_{\mathrm{r}})^{\mathrm{T}}$. $\boldsymbol{f}_{2\mathrm{f}}=\boldsymbol{f}_2+\boldsymbol{I}^{-1}M_{\mathrm{B}}$, $\boldsymbol{g}_{2\mathrm{f}}=\boldsymbol{g}_2\boldsymbol{B}$,

$$\boldsymbol{I}=\begin{pmatrix} I_{\mathrm{xx}} & 0 & -I_{\mathrm{xz}} \\ 0 & I_{\mathrm{yy}} & 0 \\ -I_{\mathrm{xz}} & 0 & I_{\mathrm{zz}} \end{pmatrix}\quad \boldsymbol{B}=\hat{q}S_{\mathrm{ref}}\boldsymbol{I}^{-1}\begin{pmatrix} b & 0 & 0 \\ 0 & c & 0 \\ 0 & 0 & b \end{pmatrix}\cdot \begin{pmatrix} C_{\mathrm{mx},\delta_{\mathrm{e}}} & C_{\mathrm{mx},\delta_{\mathrm{a}}} & C_{\mathrm{mx},\delta_{\mathrm{r}}} \\ C_{\mathrm{my},\delta_{\mathrm{e}}} & C_{\mathrm{my},\delta_{\mathrm{a}}} & C_{\mathrm{my},\delta_{\mathrm{r}}} \\ C_{\mathrm{mz},\delta_{\mathrm{e}}} & C_{\mathrm{mz},\delta_{\mathrm{a}}} & C_{\mathrm{mz},\delta_{\mathrm{r}}} \end{pmatrix}$$

When the actuator cannot operate fully, a fault factor matrix is introduced into the control input $\boldsymbol{u}_2$, then one has the dynamics of HRV with actuator failure

$$\dot{\boldsymbol{x}}_2=\boldsymbol{f}_{2\mathrm{f}}+\boldsymbol{g}_{2\mathrm{f}}\boldsymbol{u}_2-\boldsymbol{g}_{2\mathrm{f}}\boldsymbol{F}\boldsymbol{u}_2 \tag{9}$$

where $\boldsymbol{F}$ is fault factor matrix, $\boldsymbol{F}=\mathrm{diag}(F_1,F_2,F_3),(0\le F_j<1,j=1,2,3)$. When the corresponding actuator can work normally, $F_j=0(j=1,2,3)$. If $0<F_j<1(j=1,2,3)$, it means that actuator failure occurs.

1.2 Prescribed performance function

The basic knowledge of prescribed performance is recalled herein. The core idea of prescribed performance[11] is to limit the state variable, which is corresponding to the tracking error $e(t)$ in FTC problem, to a desired range to improve system performance from three aspects, viz., the convergence rate, the overshoot and the steady-state error[12]. Based on these considerations, the three indicators mentioned above can be guaranteed by a prescribed bounded performance function $\rho(t)$ and an error transformation function $\epsilon(t)$. Specifically, the tracking error $e(t)$ satisfies

$$\begin{cases} -a\rho(t)<e(t)<\rho(t), & e(t_0)>0 \\ -\rho(t)<e(t)<a\rho(t), & e(t_0)<0 \end{cases} \tag{10}$$

where $0\le a\le 1$. The graphical presentation of tracking error $e(t)$ can be illustrated in Fig.1. $e(t)$ is always changing within the prescribed performance function.

In order to realize the graphical presentation illustrated in Fig.1, the performance function $\rho(t)$ should satisfy the following conditions[11]

① $\rho(t)$ is decreasing monotonically.

② The derivatives of all orders of $\rho(t)$ exist.

③ $\rho_0=\rho(0)>0$, $\rho(t)>0$, $\lim\limits_{t\to\infty}\rho(t)=\rho_\infty$.

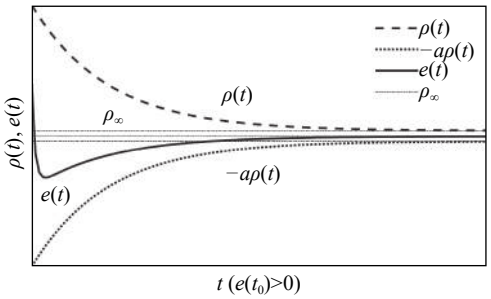

Fig. 1 Graphical presentation of $\rho(t)$

Then a candidate performance function $\rho(t)$ can be chosen with the following form[16]

$$\rho(t)=(\rho_0-\rho_\infty)e^{-\xi t}+\rho_\infty \tag{11}$$

where $\rho_0>\rho_\infty>0$, $\xi>0$.

Additionally, the error transformation function $\epsilon(t)$ is introduced to convert the constrained error into an equivalent unconstrained error as

$$\epsilon(t)=\frac{e(t)}{\rho(t)}\triangleq P(\kappa(t)) \tag{12}$$

where $\epsilon(t)$ satisfies the following conditions.

① $\epsilon(t)$ is smooth, invertible and strictly increasing.

② $\begin{cases} -a<P(\kappa(t))<1, & e(t_0)>0 \\ -1<P(\kappa(t))<a, & e(t_0)<0 \end{cases}$

③ $\begin{cases} \lim\limits_{\epsilon\to-\infty}P(\kappa(t))=-a,\ \lim\limits_{\epsilon\to+\infty}P(\kappa(t))=1, & e(t_0)>0 \\ \lim\limits_{\epsilon\to-\infty}P(\kappa(t))=-1,\ \lim\limits_{\epsilon\to+\infty}P(\kappa(t))=a, & e(t_0)<0 \end{cases}$

Thus the transformed error $\kappa(t)$ can be expressed as

$$\kappa(t)=P^{-1}(\kappa(t)) \tag{13}$$

According to the conditions of $P(\kappa(t))$, the graphical presentation of $P(\kappa(t))$ can be seen in Fig. 2.

1.3 Control objective

The fault-tolerate controller is designed to achieve that the tracking error $\boldsymbol{e}_1=(e_{11},e_{12},e_{13})^{\mathrm{T}}=\boldsymbol{x}_1-\boldsymbol{x}_{1,\mathrm{ref}}$ and $\boldsymbol{e}_2=(e_{21},e_{22},e_{23})^{\mathrm{T}}=\boldsymbol{x}_2-\boldsymbol{x}_{2,\mathrm{ref}}$ converge to a prescribed set asymptotically with faulty actuator. In other words, attitude angle $\boldsymbol{x}_1$

and angle rate $\boldsymbol{x}_2$ can track the desired value $\boldsymbol{x}_{1,\text{ref}} = (\alpha_{\text{ref}}, \beta_{\text{ref}}, \mu_{\text{ref}})^{\text{T}}$ and $\boldsymbol{x}_{2,\text{ref}} = (p_{\text{ref}}, q_{\text{ref}}, r_{\text{ref}})^{\text{T}}$ quickly and accurately when the actuator fails to work completely.

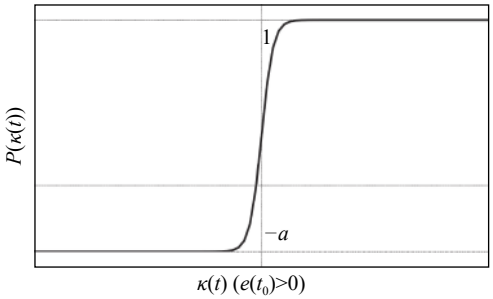

Fig. 2 Graphical presentation of $P(\kappa(t))$

2 Main Results

In this section, a fault-tolerant control scheme is designed for HRV faulty system with prescribed performance based on integral sliding mode control. Considering the HRV dynamics under actuator failure, the fault-tolerant control system consists of two controllers, that is, a robust controller for outer loop and a fault-tolerant controller for inner loop. In the outer loop, the control goal is twofold, forcing attitude angle α, β, μ to follow the desired command and providing $p_{\text{ref}}, q_{\text{ref}}, r_{\text{ref}}$ for inner loop. Then the goal of fault-tolerant control pursued in inner loop is to force the tracking error $\boldsymbol{e}_2$ converge to a prescribed set asymptotically with the loss of actuator effectiveness failure.

2.1 Error transformation

In this subsection, prescribed performance function $\rho(t)$ is chosen with the same form as Eq. (11). To meet the controller design in this topic, $\rho(t)$ is expressed as $\rho_{ij}(t)(i = 1, 2; j = 1, 2, 3)$

$$\rho_{ij}(t) = (\rho_{ij0} - \rho_{ij\infty})e^{-\xi_{ij}t} + \rho_{ij\infty} \tag{14}$$

where $\rho_{ij0} > \rho_{ij\infty} > 0(i = 1, 2;\ j = 1, 2, 3)$, $\xi_{ij} > 0$ $(i = 1, 2;\ j = 1, 2, 3)$. The relation between error transformation function and error is

$$\epsilon_{ij}(t) = \frac{e_{ij}(t)}{\rho_{ij}(t)} \triangleq P_{ij}(\kappa_{ij}(t))(i = 1, 2; j = 1, 2, 3) \tag{15}$$

Then a new error transformation function $P_{ij}(\kappa_{ij}(t))(i = 1, 2; j = 1, 2, 3)$ motivated by Sigmoid function is given. Different from the original sigmoid function, a parameter $a_{ij}(i = 1, 2; j = 1, 2, 3)$ is introduced. Then one has the error transformation function $P_{ij}(\kappa_{ij}(t))(i = 1, 2; j = 1, 2,3)$

$$P_{ij}(\kappa_{ij}(t)) = \begin{cases} \dfrac{1 - a_{ij}e^{-\kappa_{ij}(t)}}{1 + e^{-\kappa_{ij}(t)}}, & e_{ij}(t_0) > 0 \\ \dfrac{a_{ij} - e^{-\kappa_{ij}(t)}}{1 + e^{-\kappa_{ij}(t)}}, & e_{ij}(t_0) < 0 \end{cases}$$
$$(i = 1, 2; j = 1, 2, 3) \tag{16}$$

Clearly, $P_{ij}(\kappa_{ij}(t))(i = 1, 2;\ j = 1, 2, 3)$ satisfies the conditions. Then the transformed error $\kappa_{ij}(t)(i = 1, 2;\ j = 1, 2, 3)$ is obtained as

$$\kappa_{ij}(t) = \begin{cases} \ln \dfrac{\epsilon_{ij}(t) + a_{ij}}{1 - \epsilon_{ij}(t)}, & e_{ij}(t_0) > 0 \\ \ln \dfrac{\epsilon_{ij}(t) + 1}{a_{ij} - \epsilon_{ij}(t)}, & e_{ij}(t_0) < 0 \end{cases}$$
$$(i = 1, 2; j = 1, 2, 3) \tag{17}$$

2.2 Integral sliding mode controller for outer loop

An integral sliding mode robust controller and integral sliding mode fault-tolerant controller are designed for HRV in this subsection. At first, distinguished from the previous integral sliding mode control, sliding mode variable is no longer the tracking error $\boldsymbol{e}_1$ and $\boldsymbol{e}_2$ but the corresponding transformed error $\boldsymbol{\kappa}_1 = (\kappa_{11}(t), \kappa_{12}(t), \kappa_{13}(t))^{\text{T}}$ and $\boldsymbol{\kappa}_2 = (\kappa_{21}(t), \kappa_{22}(t), \kappa_{23}(t))^{\text{T}}$.

Thus, the integral sliding mode manifold $\boldsymbol{s}_i = (s_{i1}(t), s_{i2}(t), s_{i3}(t))^{\text{T}}, i = 1, 2$ and reaching law $\dot{\boldsymbol{s}}_i = (\dot{s}_{i1}(t), \dot{s}_{i2}(t), \dot{s}_{i3}(t))^{\text{T}}(i = 1, 2)$ for each loop are designed as

$$s_{ij}(t) = \kappa_{ij}(t) + c_{ij}\int_0^t \kappa_{ij}(\iota)d\iota(i = 1, 2; j = 1, 2, 3) \tag{18}$$

$$\dot{s}_{ij}(t) = -\tau_{ij}s_{ij}(t) - \eta_{ij}\text{sgn}(s_{ij}(t))(i = 1, 2; j = 1, 2, 3) \tag{19}$$

The derivative of $s_{ij}(t)(i = 1, 2;\ j = 1, 2, 3)$ in Eq. (18) can be derived as

$$\dot{s}_{ij}(t) = \dot{\kappa}_{ij}(t) + c_{ij}\kappa_{ij}(t)(i = 1, 2; j = 1, 2, 3) \tag{20}$$

Substituting the reaching law (19) into Eq. (20), we can obtain that

$$\dot{\kappa}_{ij}(t) + c_{ij}\kappa_{ij}(t) = -\tau_{ij}s_{ij}(t) - \eta_{ij}\text{sgn}(s_{ij}(t))$$
$$(i = 1, 2; j = 1, 2, 3) \tag{21}$$

Apparently, $\dot{\epsilon}_{ij}(t)(i=1,2;\ j=1,2,3)$ and $\dot{\kappa}_{ij}(t)$ $(i=1,2;\ j=1,2,3)$ can be calculated easily as

$$\dot{\epsilon}_{ij}(t)=\frac{\dot{e}_{ij}(t)\rho_{ij}(t)-e_{ij}(t)\dot{\rho}_{ij}(t)}{\rho_{ij}^2(t)}\ (i=1,2;\ j=1,2,3) \tag{22}$$

$$\dot{\kappa}_{ij}(t)=\begin{cases}\dfrac{\dot{\epsilon}_{ij}(t)(a_{ij}+1)}{(\epsilon_{ij}(t)+a_{ij})(1-\epsilon_{ij}(t))}, & e_{ij}(t_0)>0\\ \dfrac{\dot{\epsilon}_{ij}(t)(a_{ij}+1)}{(\epsilon_{ij}(t)+1)(a_{ij}-\epsilon_{ij}(t))}, & e_{ij}(t_0)<0\end{cases}\quad (i=1,2;\ j=1,2,3) \tag{23}$$

Then the outer-loop robust controller $\boldsymbol{u}_1=(u_{11}(t),u_{12}(t),u_{13}(t))^{\mathrm{T}}$ and the inner-loop fault-tolerant controller $\boldsymbol{u}_2=(u_{21}(t),u_{22}(t),u_{23}(t))^{\mathrm{T}}$ can be obtained using the reaching law method as

$$\boldsymbol{u}_1=\begin{cases}\dfrac{1}{\boldsymbol{R}(\boldsymbol{x}_1)}(\dot{\boldsymbol{x}}_{1c}+\epsilon_1\dot{\boldsymbol{\rho}}_1+\dfrac{\boldsymbol{\rho}_1(\epsilon_1+\boldsymbol{A}_1)(\boldsymbol{E}-\epsilon_1)}{(\boldsymbol{E}+\boldsymbol{A}_1)}\\ (-\tau_1\boldsymbol{s}_1-\boldsymbol{\eta}_1\mathbf{SGN}_1-\boldsymbol{C}_1\boldsymbol{\kappa}_1)),\\ e_{1\mathrm{j}}(t_0)>0\\ \dfrac{1}{\boldsymbol{R}(\boldsymbol{x}_1)}(\dot{\boldsymbol{x}}_{1c}+\epsilon_1\dot{\boldsymbol{\rho}}_1+\dfrac{\boldsymbol{\rho}_1(\epsilon_1+\boldsymbol{E})(\boldsymbol{A}_1-\epsilon_1)}{(\boldsymbol{E}+\boldsymbol{A}_1)}\\ (-\tau_1\boldsymbol{s}_1-\boldsymbol{\eta}_1\mathbf{SGN}_1-\boldsymbol{C}_1\boldsymbol{\kappa}_1)),\\ e_{1\mathrm{j}}(t_0)<0\end{cases} \tag{24}$$

$$\boldsymbol{u}_2=\begin{cases}\dfrac{1}{\boldsymbol{g}_{2\mathrm{f}}}(\dot{\boldsymbol{x}}_{2c}+\epsilon_2\dot{\boldsymbol{\rho}}_2+\dfrac{\boldsymbol{\rho}_2(\epsilon_2+\boldsymbol{A}_2)(\boldsymbol{E}-\epsilon_2)}{(\boldsymbol{E}+\boldsymbol{A}_2)}\\ (-\boldsymbol{\tau}_2\boldsymbol{s}_2-\boldsymbol{\eta}_2\mathbf{SGN}_2-\boldsymbol{C}_2\boldsymbol{\kappa}_2)-\boldsymbol{f}_{2\mathrm{f}}+\boldsymbol{g}_{2\mathrm{f}}\boldsymbol{F}\boldsymbol{u}_2),\\ e_{2j}(t_0)>0\\ \dfrac{1}{\boldsymbol{g}_{2\mathrm{f}}}(\dot{\boldsymbol{x}}_{2c}+\epsilon_2\dot{\boldsymbol{\rho}}_2+\dfrac{\boldsymbol{\rho}_2(\epsilon_2+\boldsymbol{E})(\boldsymbol{A}_2-\boldsymbol{E})}{(\boldsymbol{E}+\boldsymbol{A}_2)}\\ (-\boldsymbol{\tau}_2\boldsymbol{s}_2-\boldsymbol{\eta}_2\mathbf{SGN}_2-\boldsymbol{C}_2\boldsymbol{\kappa}_2)-\boldsymbol{f}_{2\mathrm{f}}+\boldsymbol{g}_{2\mathrm{f}}\boldsymbol{F}\boldsymbol{u}_2),\\ e_{2j}(t_0)<0\end{cases} \tag{25}$$

in which $i=1,\ 2$ and $j=1,\ 2,\ 3$.

$\eta_{1j}\geq\max\left\{\left|\dfrac{(a_{1j}+1)}{\rho_{1j}(\epsilon_{1j}+a_{1j})(1-\epsilon_{1j})}\bar{d}_j\right|,\left|\dfrac{(a_{1j}+1)}{\rho_{1j}(\epsilon_{1j}+1)(a_{1j}-\epsilon_{1j})}\bar{d}_j\right|\right\}$

$\eta_{2j}>0$. $\bar{d}_j$ is the upper bound of d_j .

$\boldsymbol{s}_i=(s_{i1}(t),s_{i2}(t),s_{i3}(t))^{\mathrm{T}}$, $\boldsymbol{\tau}_i=\mathrm{diag}(\tau_{i1},\tau_{i2},\tau_{i3})$,

$\boldsymbol{C}_i=\mathrm{diag}(c_{i1},c_{i2},c_{i3})$, $\dot{\boldsymbol{\rho}}_i=(\dot{\rho}_{i1}(t),\dot{\rho}_{i2}(t),\dot{\rho}_{i3}(t))^{\mathrm{T}}$,

$\boldsymbol{\eta}_i=\mathrm{diag}(\eta_{i1},\eta_{i2},\eta_{i3})$, $\boldsymbol{A}_i=\mathrm{diag}(a_{i1},a_{i2},a_{i3})$,

$\boldsymbol{\rho}_i=\mathrm{diag}(\rho_{i1}(t),\rho_{i2}(t),\rho_{i3}(t))$,

$\boldsymbol{\kappa}_i=(\kappa_{i1}(t),\kappa_{i2}(t),\kappa_{i3}(t))^{\mathrm{T}}$,

$\epsilon_i=\mathrm{diag}(\epsilon_{i1}(t),\epsilon_{i2}(t),\epsilon_{i3}(t))$, $\boldsymbol{E}=\mathrm{diag}(1,1,1)$,

$\mathbf{SGN}_i=(\mathrm{sgn}(s_{i1}(t)),\mathrm{sgn}(s_{i2}(t)),\mathrm{sgn}(s_{i3}(t)))^{\mathrm{T}}$.

The first result is given in Theorem 1.

Theorem 1 For outer-loop nonlinear system (3), based on transformed error (17), sliding mode manifold (18) and reaching law (19), the integral sliding mode robust controller (24) is designed to ensure that the tracking error $\boldsymbol{e}_1$ can converge to a prescribed set asymptotically.

Proof A candidate Lyapunov function V_1 is chosen as

$$V_1=0.5\boldsymbol{s}_1^{\mathrm{T}}\boldsymbol{s}_1 \tag{26}$$

It is worthy to note that there are two cases in Eqs. (23) (24). Since the analysis processes in the two cases are in a very similar manner, for the limited space we prove the case $e(t_0)>0$ only.

Firstly, differentiating (26) and substituting (20) into the derivation yields

$$\dot{V}_1=\boldsymbol{s}_1^T(\dot{\boldsymbol{\kappa}}_1+\boldsymbol{C}_1\boldsymbol{\kappa}_1) \tag{27}$$

Substitute Eqs. (17) (22) (23) into Eq. (27) and define $\mathbf{Mid}_1$ and $\mathbf{Mid}_2$ as

$$\mathbf{Mid}_1\triangleq\mathrm{diag}\left(\frac{\dot{e}_{11}(t)(a_{11}+1)}{\rho_{11}(t)(\epsilon_{11}(t)+a_{11})(1-\epsilon_{11}(t))},\frac{\dot{e}_{12}(t)(a_{12}+1)}{\rho_{12}(t)(\epsilon_{12}(t)+a_{12})(1-\epsilon_{12}(t))},\frac{\dot{e}_{13}(t)(a_{13}+1)}{\rho_{13}(t)(\epsilon_{13}(t)+a_{13})(1-\epsilon_{13}(t))}\right) \tag{28}$$

$$\mathbf{Mid}_2\triangleq\left(\frac{-\epsilon_{11}(t)\dot{\rho}_{11}(t)(a_{11}+1)}{\rho_{11}(t)(\epsilon_{11}(t)+a_{11})(1-\epsilon_{11}(t))},\frac{-\epsilon_{12}(t)\dot{\rho}_{12}(t)(a_{12}+1)}{\rho_{12}(t)(\epsilon_{12}(t)+a_{12})(1-\epsilon_{12}(t))},\frac{-\epsilon_{13}(t)\dot{\rho}_{13}(t)(a_{13}+1)}{\rho_{13}(t)(\epsilon_{13}(t)+a_{13})(1-\epsilon_{13}(t))}\right)^{\mathrm{T}} \tag{29}$$

Meanwhile, substitute Eqs. (3) (28) (29) and controller (24) into Eq. (27), it can be obtained that

$$\begin{aligned}\dot{V}_1=&s_1^{\mathrm{T}}(\mathbf{Mid}_1\cdot\boldsymbol{D}+(-\tau_1\boldsymbol{s}_1-\boldsymbol{\eta}_1\mathbf{SGN}_1))=\\ &-\sum_{j=1}^{3}\tau_{1j}s_{1j}^2(t)+\sum_{j=1}^{3}s_{1j}(t)\\ &\left(\frac{\dot{e}_{1j}(t)(a_{1j}+1)}{\rho_{1j}(t)(\epsilon_{1\mathrm{j}}(t)+a_{1j})(1-\epsilon_{1j}(t))}d_j-\right.\\ &\left.\eta_{1j}\mathrm{sgn}(s_{1\mathrm{j}}(t))\right)\leq 0\end{aligned} \tag{30}$$

Thus the inequality $\dot{V}_1<0$ holds. Therefore, $s_{1j}(t)(j=1,\ 2,\ 3)$ will converge to zero asymptot-

ically. According to Eq. (18), we have

$$\dot{\kappa}_{ij}(t)+c_{ij}\kappa_{ij}(t)=0\ (i=1,\ 2,\ j=1,\ 2,\ 3) \tag{31}$$

Then a Lyapunov candidate is chosen as

$$V_{\kappa}=\frac{1}{2}\kappa_{ij}^{2}(t)\ (i=1,\ 2,\ j=1,\ 2,\ 3) \tag{32}$$

Taking derivation of Eq. (32) yields

$$\dot{V}_{\kappa}=\kappa_{ij}(t)\dot{\kappa}_{ij}(t)\ (i=1,\ 2,\ j=1,\ 2,\ 3) \tag{33}$$

Substituting Eq. (31) into Eq. (32) yields

$$\begin{aligned}&\dot{V}_{\kappa}=\kappa_{ij}(t)(-c_{ij}\kappa_{ij}(t))=-c_{ij}\kappa_{ij}^{2}(t)\leq 0\\&(i=1,\ 2,\ j=1,\ 2,\ 3)\end{aligned} \tag{34}$$

Therefore $\kappa_{ij}(t)(i=1,\ 2,\ j=1,\ 2,\ 3)$ can converge to zero asymptotically. Then we would take the scenario $e_{ij}(t_0)>0(i=1,\ 2,\ j=1,\ 2,\ 3)$ as an example to illustrate the convergence of $e_{ij}(t)(i=1,\ 2,\ j=1,\ 2,\ 3)$.

Firstly, rewrite error transformation $P_{ij}(\kappa_{ij}(t))$ $(i=1,\ 2,\ j=1,\ 2,\ 3)$ as follows

$$P_{ij}(\kappa_{ij})=\frac{1-a_{ij}e^{-\kappa ij}}{1+e^{-\kappa ij}},e_{ij}(t_0)>0(i=1,2,j=1,2,3) \tag{35}$$

When $\kappa_{ij}(t)(i=1,\ 2,\ j=1,\ 2,\ 3)$ converge to zero, Eq. (35) turns to

$$P_{ij}(\kappa_{ij}(t))=\frac{1-a_{ij}}{2},e_{ij}(t_0)>0(i=1,2,j=1,2,3) \tag{36}$$

According to the error transformation function $\epsilon_{ij}(t)(i=1,\ 2,\ j=1,\ 2,\ 3)$, one has

$$e_{ij}(t)=\frac{1-a_{ij}}{2}\rho_{ij}(t),e_{ij}(t_0)>0(i=1,\ 2,\ j=1,\ 2,\ 3) \tag{37}$$

Then tracking error $e_{ij}(t)(e_{ij}(t_0)>0\ (i=1,\ 2,\ j=1,\ 2,\ 3)$ converge to the prescribed set. This completes the proof.

2.3 Integral sliding mode fault-tolerant controller for inner loop

Considering the controller (25), the final term $\boldsymbol{g}_{2\mathrm{f}}\boldsymbol{F}\boldsymbol{u}_2$ is unknown. In other words, when the actuator fails to work fully, controller $\boldsymbol{u}_2$ is hardly to obtain. To solve this problem, $\boldsymbol{g}_{2\mathrm{f}}\boldsymbol{F}\boldsymbol{u}_2$ is regarded as unknown disturbance and an ESO[19] is adopted to estimate the disturbance as the fault compensation mechanism. Firstly, defining $\boldsymbol{y}_1=\boldsymbol{x}_2$, $\boldsymbol{y}_2=-\boldsymbol{g}_{2\mathrm{f}}\boldsymbol{F}\boldsymbol{u}_2$, then rewrite Eq. (4) as

$$\begin{cases}\dot{\boldsymbol{y}}_1=\boldsymbol{f}_{2\mathrm{f}}(\boldsymbol{y}_1)+\boldsymbol{g}_{2\mathrm{f}}(\boldsymbol{y}_1)\boldsymbol{u}_2+\boldsymbol{y}_2\\ \dot{\boldsymbol{y}}_2=\boldsymbol{v}(t)\end{cases} \tag{38}$$

where $\boldsymbol{v}(t)=(\varpi_1,\varpi_2,\varpi_3)^{\mathrm{T}}$ is the derivate of $\boldsymbol{y}_2$. Define the state variable $\boldsymbol{z}_1$ and $\boldsymbol{z}_2$ to construct the ESO for (38) as follows

$$\begin{cases}\dot{\boldsymbol{z}}_1=\boldsymbol{z}_2-\boldsymbol{\beta}_1(\boldsymbol{z}_1-\boldsymbol{y}_1)+\boldsymbol{f}_{2\mathrm{f}}(\boldsymbol{y}_1)+\boldsymbol{g}_{2\mathrm{f}}(\boldsymbol{y}_1)\boldsymbol{u}_2\\ \dot{\boldsymbol{z}}_2=-\boldsymbol{\beta}_2\mathbf{Fal}(\varepsilon_{1j},b_j,\delta_{\mathrm{j}})\end{cases} \tag{39}$$

in which $\boldsymbol{\beta}_i=\mathrm{diag}(\beta_{i1},\ \beta_{i2},\ \beta_{i3})$ $(\beta_{ij}>0,\ i=1,\ 2,\ j=1,\ 2,\ 3)$ is the parameters in ESO. $\mathbf{Fal}(\varepsilon_{1j},\ b_j,\ \delta_j)=(\mathrm{Fal}_1(\varepsilon_{11},\ b_1,\ \delta_1),\ \mathrm{Fal}_2(\varepsilon_{12},\ b_2,\ \delta_2),\ \mathrm{Fal}_3(\varepsilon_{13},\ b_3,\ \delta_3))^{\mathrm{T}}$

$$\mathrm{Fal}_j(\varepsilon_{1j},b_j,\delta_j)=\begin{cases}\varepsilon_{1j}\delta_j^{\,b_j-1}, & |\varepsilon_{1j}|\leq\delta_j\\ |\varepsilon_{1j}|^{b_j}\mathrm{sgn}(\varepsilon_{1j}), & |\varepsilon_{1j}|>\delta_j\end{cases}(j=1,2,3) \tag{40}$$

in which, $\varepsilon_{1j}=z_j-y_j(j=1,2,3)$. $\delta_j>0(j=1,\ 2,\ 3)$ and $0<b_j<1(j=1,2,3)$.

Then we discuss the convergence of ESO (39). The estimation error can be defined as $\boldsymbol{\varepsilon}_1=\boldsymbol{z}_1-\boldsymbol{y}_1=(\varepsilon_{11},\varepsilon_{12},\varepsilon_{13})^{\mathrm{T}}$ and $\boldsymbol{\varepsilon}_2=\boldsymbol{z}_2-\boldsymbol{y}_2=(\varepsilon_{21},\varepsilon_{22},\varepsilon_{23})^{\mathrm{T}}$, it can be obtained that

$$\begin{cases}\dot{\boldsymbol{\varepsilon}}_1=-\boldsymbol{\beta}_1\boldsymbol{\varepsilon}_1+\boldsymbol{\varepsilon}_2\\ \dot{\boldsymbol{\varepsilon}}_2=-\boldsymbol{\beta}_2\mathbf{Fal}(\varepsilon_j,b_j,\delta_j)+\boldsymbol{v}(t)\end{cases} \tag{41}$$

Based on the analysis in Ref. [20] for the stability of ESO, the following condition must be satisfied

$$\beta_{2j}<\frac{1}{4}\delta_j^{1-b_j}\beta_{1j}^{2}(j=1,2,3) \tag{42}$$

Then the ESO is stable and $\boldsymbol{\varepsilon}_i(i=1,2)\to 0$ holds. Therefore the ESO (39) provides the estimation value of $\boldsymbol{y}_2$. Then the fault-tolerant control can be obtained as follows

$$\boldsymbol{u}_{ftc}=\begin{cases}\dfrac{1}{\boldsymbol{g}_{2\mathrm{f}}}\Big(\dot{\boldsymbol{x}}_{2\mathrm{c}}+{}_2\dot{\boldsymbol{\rho}}_2+\dfrac{\boldsymbol{\rho}_2(\epsilon_2+\boldsymbol{A}_2)(\boldsymbol{E}-\epsilon_2)}{(E+\boldsymbol{A}_2)}\\ (-\boldsymbol{\tau}_2\boldsymbol{s}_2-\boldsymbol{\eta}_2\mathbf{SGN}_2-\boldsymbol{C}_2\boldsymbol{\kappa}_2)-\boldsymbol{f}_{2\mathrm{f}}+\boldsymbol{z}_2),\\ e_{2j}(t_0)>0\\ \dfrac{1}{\boldsymbol{g}_{2\mathrm{f}}}\Big(\dot{\boldsymbol{x}}_{2c}+\epsilon_2\dot{\boldsymbol{\rho}}_2+\dfrac{\boldsymbol{\rho}_2(\epsilon_2+\boldsymbol{E})(\boldsymbol{A}_2-\boldsymbol{E})}{(\boldsymbol{E}+\boldsymbol{A}_2)}\\ (-\boldsymbol{\tau}_2\boldsymbol{s}_2-\boldsymbol{\eta}\epsilon_2\mathbf{SGN}_2-\boldsymbol{C}_2\boldsymbol{\kappa}_2)-\boldsymbol{f}_{2\mathrm{f}}+\boldsymbol{z}_2),\\ e_{2j}(t_0)<0\end{cases}\quad(j=1,2,3) \tag{43}$$

The second result is given in Theorem 2.

Theorem 2 For inner-loop nonlinear system (4), based on transformed error (17), sliding mode manifold (18) and reaching law (19), the integral sliding mode fault-tolerant controller (43) is designed to ensure that the tracking error $\boldsymbol{e}_2$ can converge to a prescribed set asymptotically.

Proof A candidate Lyapunov function V_2 is chosen as

$$V_2 = 0.5\boldsymbol{s}_2^{\mathrm{T}}\boldsymbol{s}_2 \tag{44}$$

It is worthy to note that there are two cases in Eqs. (23) (24). Since the analysis processes in the two cases are in a very similar manner, for the limited space we prove the case $e(t_0) > 0$ only.

Firstly, differentiating Eq. (44) and substituting Eq. (20) into the derivation yield

$$\dot{V}_2 = \boldsymbol{s}_2^{\mathrm{T}}(\dot{\boldsymbol{\kappa}}_2 + \boldsymbol{C}_2\boldsymbol{\kappa}_2) \tag{45}$$

Substituting Eqs. (17) (22) (23) into Eq. (45), it can be deduced that

$$\begin{aligned}\dot{V}_2 =& \boldsymbol{s}_2^{\mathrm{T}}(\mathbf{Mid}_3 \cdot \dot{\boldsymbol{x}}_2 - \mathbf{Mid}_3 \cdot \dot{\boldsymbol{x}}_{2,\mathrm{ref}} + \mathbf{Mid}_4 + \boldsymbol{C}_2\boldsymbol{\kappa}_2) = \\ & -\sum_{j=1}^{3}(\tau_{2j}s_{2j}^2 + \eta_{2j}|s_{2j}|) + \boldsymbol{s}_2^{\mathrm{T}}\mathbf{Mid}_3 \cdot \boldsymbol{\varepsilon}_2\end{aligned} \tag{46}$$

in which

$$\begin{aligned}\mathbf{Mid}_3 \triangleq \mathrm{diag}\Bigg(&\frac{\dot{e}_{21}(a_{21}+1)}{\rho_{21}(\epsilon_{21}+a_{21})(1-\epsilon_{21})},\\ &\frac{\dot{e}_{22}(a_{22}+1)}{\rho_{22}(\epsilon_{22}+a_{22})(1-\epsilon_{22})}, \frac{\dot{e}_{23}(a_{23}+1)}{\rho_{23}(\epsilon_{23}+a_{23})(1-\epsilon_{23})}\Bigg)\end{aligned} \tag{47}$$

$$\begin{aligned}\mathbf{Mid}_4 \triangleq \Bigg(&\frac{-\epsilon_{21}\dot{\rho}_{21}(a_{21}+1)}{\rho_{21}(\epsilon_{21}+a_{21})(1-\epsilon_{21})},\\ &\frac{-\epsilon_{22}\dot{\rho}_{22}(a_{22}+1)}{\rho_{22}(\epsilon_{22}+a_{22})(1-\epsilon_{22})}, \frac{-\epsilon_{23}\dot{\rho}_{23}(a_{23}+1)}{\rho_{23}(\epsilon_{23}+a_{23})(1-\epsilon_{23})}\Bigg)^{\mathrm{T}}\end{aligned} \tag{48}$$

Since the estimation error $\boldsymbol{\varepsilon}_2 \to 0$, it can be obtained that $\dot{V}_2 < 0$. As a result, sliding mode manifold $s_{2j}(j = 1, 2, 3)$ will converge to zero. By Eq. (15), the tracking error $e_{2j}(j = 1, 2, 3)$ converges to a prescribed set. The analysis process of the convergence of $e_{2j}(j = 1, 2, 3)$ is in a very similar manner with that in Theorem 1, for the limited space it is omitted here. This completes the proof.

3 Simulation

In this section, numerical simulations are given to verify the effectiveness of robust controller (24) and fault-tolerant controller (43) for HRV attitude control in reentry flight phase. Failure factor F_j $(j = 1, 2, 3)$ is assigned $F_j = 0.35$ $(j = 1, 2, 3)$. The initial conditions are given as: $\alpha(0) = 5°$, $\beta(0) = 0.1°$, $\mu(0) = 3°$, $p(0) = 0.01(°)/\mathrm{s}$, $q(0) = 0.01(°)/\mathrm{s}$, $r(0) = 0.01(°)/\mathrm{s}$, $V(0) = 3\,000\ \mathrm{m}\cdot\mathrm{s}^{-1}$. Other configurations can be seen in Ref.[16]. Reference order is $\boldsymbol{x}_{1,\mathrm{ref}} = (3°, 0°, 1°)^{\mathrm{T}}$. Parameters used herein are listed in Tab 1.

Tab. 1 Parameters of controllers, ESO and prescribed performance function

Parameter	Numerical value	Parameter	Numerical value
ρ_{110}, ρ_{120}, ρ_{130}	4, 0.4, 4	τ_1	diag (1.65, 1.5, 1.5)
ρ_{210}, ρ_{220}, ρ_{230}	6, 12, 0.6	τ_2	diag (7.5, 5, 25)
$\rho_{ij\infty}$	0.02	c_{1j}	0.1
ξ_{1j}	0.5	c_{2j}	0.01
ξ_{2j}	0.3	β_{1j}	220
a_{ij}	0.98	β_{2j}	900
b_j	0.6	δ_j	0.01

The simulation results are illustrated in Figs. 3–8. Fig. 3 and Fig. 4 show that when failure occurs at $t = 12$ s and the fault compensation mechanism cannot be activated immediately, the sliding mode function $s_{ij}(i = 1, 2, j = 1, 2, 3)$ cannot converge to zero. Also, when the fault-tolerant controller (43) works at $t = 22$ s, $s_{ij}(i = 1, 2, j = 1, 2, 3)$ converges to zero quickly. Figs. 5-8 show the simulation results when the actuator cannot work fully at $t = 12$ s and the fault compensation mechanism is adopted promptly. Obviously, the tracking error $\boldsymbol{e}_1$ and $\boldsymbol{e}_2$ can converge to a prescribed set asymptotically (Figs. 5–6). Besides, $\boldsymbol{e}_1$ and $\boldsymbol{e}_2$ change within the prescribed limited range all the time. Fig. 7 shows that the deflection of rudder occurs unexpected jumping due to the actuator failure. Obviously, with the help of controller $\boldsymbol{u}_2$ (44), the curve of $\delta_{\mathrm{e}}, \delta_{\mathrm{a}}, \delta_{\mathrm{r}}$ tend to be smooth in short time. As for the convergence of the observer (39), it is shown from Fig. 8 that the estimation error $\varepsilon_{2j}(j = 1, 2, 3) \to 0$ quickly.

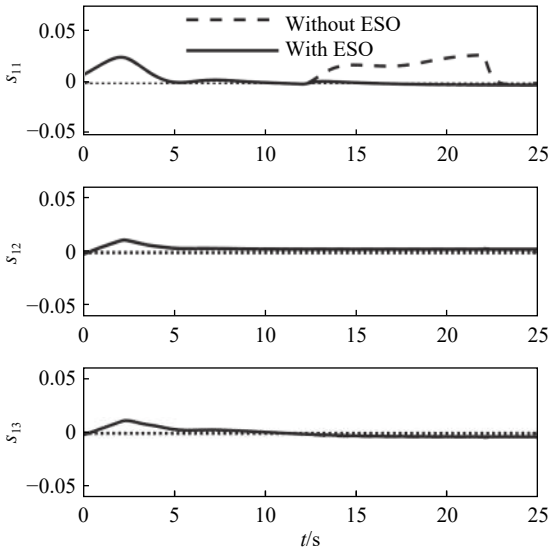

Fig. 3 Sliding surface of outer loop

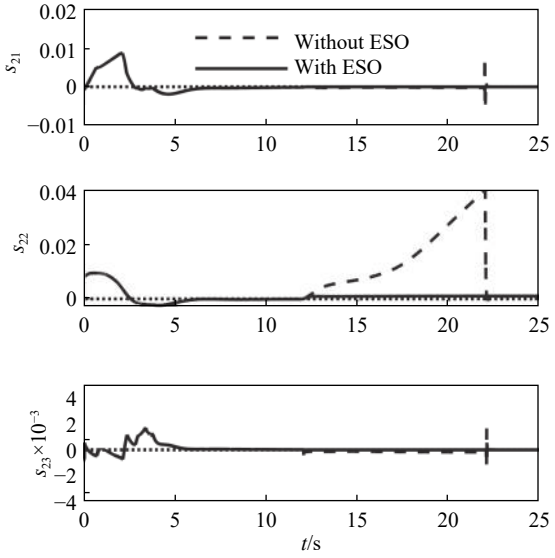

Fig. 4 Sliding surface of inner loop

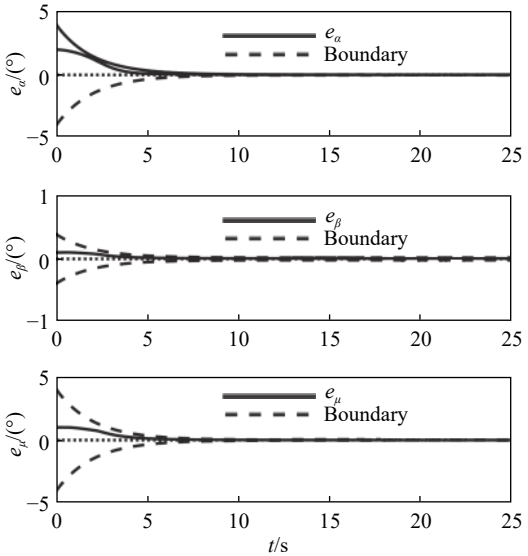

Fig. 5 Tracking error of attitude angle

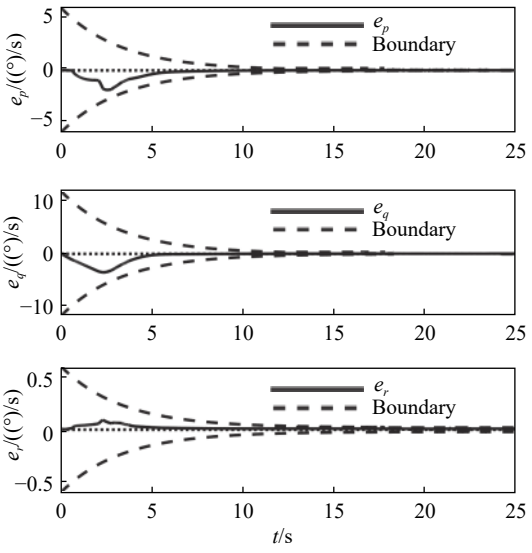

Fig. 6 Tracking error of angle rate

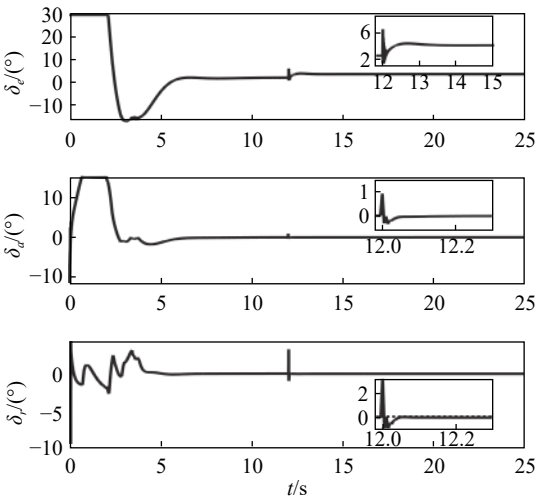

Fig. 7 Aerodynamic surface deflections

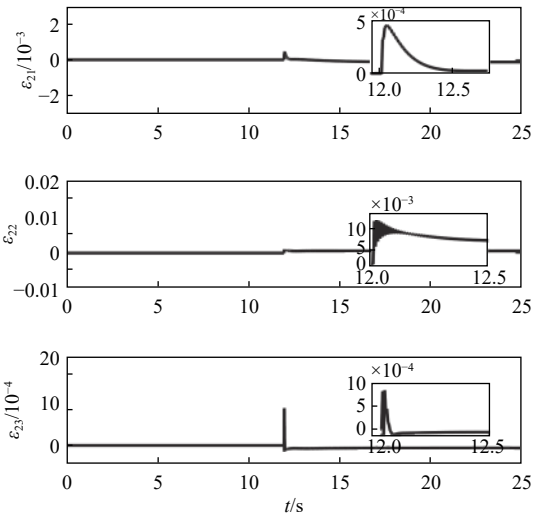

Fig. 8 Estimation error of ESO

4 Conclusion

In this paper, based on integral sliding mode control, both robust controller and fault-tolerant controller are cooperated to accomplish attitude control of HRV faulty system under actuator failure. With the proposed controller strategies, the faulty HRV system can realize attitude tracking, meanwhile, the transient process and steady state behavior of the closed-loop system can be guaranteed benefiting from PPF and ESO. Furthermore, simulation results illustrate the theoretical analysis. Our future work will be devoted to other types of failures, such as actuator stuck and actuator saturation.

References:

[1] Zhang Y, Jiang J. Bibliographical review on reconfigurable fault-tolerant control systems [J]. Annual Reviews in Control, 2008, 32(2): 229-252.

[2] Zhai R Y, Qi R Y, Jiang B. Adaptive sliding mode fault-tolerant control for hypersonic vehicle based on radial basis function neural networks [J]. International Journal of Advanced Robotic Systems, 2017, 14(3): 1-11.

[3] An H, Liu J X, Wang C H, et al. Approximate back-stepping fault-tolerant control of the flexible air-breathing hypersonic vehicle [J]. IEEE/ASME Transactions on Mechatronics, 2016, 21(3): 1680-1691.

[4] Hu X X, Karimi H R, Wu L G, et al. Model predictive control-based non-linear fault tolerant control for air-breathing hypersonic vehicles [J]. Control Theory & Applications IET, 2014, 8(13): 1147-1153.

[5] Shen Q K, Jiang B, Cocquempot V. Fuzzy logic system-based adaptive fault tolerant control for near space vehicle attitude dynamics with actuator faults [J]. IEEE Transactions on Fuzzy Systems, 2013, 21(2): 289-300.

[6] Wang T, Xie W F, Zhang Y M. Sliding mode fault tolerant control dealing with modeling uncertainties and actuator faults [J]. ISA Transactions, 2012, 51(3): 386-392.

[7] Zhang Y, Tang S J, Guo J. Adaptive-gain fast super-twisting sliding mode fault tolerant control for a reusable launch vehicle in reentry phase [J]. ISA Transactions, 2017, 71(Pt 2): 380-390.

[8] Li P, Yu X, Zhang Y, et al. Adaptive multivariable integral TSMC of a hypersonic gliding vehicle with actuator faults and model uncertainties [J]. IEEE/ASME Transactions on Mechatronics, 2017, 22(6): 2723-2735.

[9] Ming C, Sun R S, Zhu B. Nonlinear fault-tolerant control with prescribed performance for air-breathing supersonic missiles [J]. Journal of Spacecraft & Rockets, 2017, 54(5): 1092-1099.

[10] Zhao J, Jiang B, Shi P, et al. Adaptive dynamic sliding mode control for near space vehicles under actuator faults [J]. Circuits Systems & Signal Processing, 2013, 32(5): 2281-2296.

[11] Bechlioulis C P, Rovithakis G A. Prescribed performance adaptive control of SISO feedback linearizable systems with disturbances[C]//Mediterranean Conference on Control and Automation, 2008: 1035-1040.

[12] Bechlioulis C P, Rovithakis G A. Robust adaptive control of feedback linearizable MIMO nonlinear systems with prescribed performance [J]. IEEE Transactions on Automatic Control, 2008, 53(9): 2090-2099.

[13] Liu J X, An H, Gao Y B, et al. Adaptive control of hypersonic flight vehicles with limited angle-of-attack [J]. IEEE/ASME Transactions on Mechatronics, 2018, 23(2): 883-894.

[14] Liu Y J, Zeng Q, Tong S, et al. Actuator failure compensation-based adaptive control of active suspension systems with prescribed performance [J]. IEEE Transactions on Industrial Electronics, 2019, 67(8): 7044-7053.

[15] Li X G, Li G, Zhao Y, et al. Fuzzy-approximation-based prescribed performance control of air-breathing hypersonic vehicles with input constraints [J]. Science Progress, 2019, 103(1): 1-40.

[16] Shaughnessy J D, Pinckney S Z, McMinn J D. Hypersonic vehicle simulation model: Winged-cone configuration, NASA-TM-102610[R]. USA: NASA Langley Research Center, 1990.

[17] Zhang J, Wang M. A nonlinear constraint control method for reentry hypersonic vehicles [J]. Aerospace Control and Application, 2011(6): 35-40.

[18] Recasens J, Chu Q, Mulder J. Robust model predictive control of a feedback linearized system for a lifting-body re-entry vehicle[C]//Proceedings of AIAA Guidance, Navigation, and Control Conference and Exhibit. California: AIAA, 2005: 6147.

[19] Han J Q, Zhang R. Error analysis of the second order ESO [J]. Journal of Systems Science and Mathematical Sciences, 1999(4): 465-471.

[20] Wang W W, Gao Z Q. A comparison study of advanced state observer design techniques[C]//Proceedings of American Control Conference, 2003(6): 4754-4759.